AMERICAN SOCIETY FOR MICROBIOLOGY | Applied and Environmental Microbiology®

PLANT MICROBIOLOGY

RasI/R Quorum Sensing System Controls the Virulence of *Ralstonia solanacearum* Strain EP1

Jinli Yan,[a] Peng Li,[b] Xiaoqing Wang,[a] Minya Zhu,[a] Hongyu Shi,[a] Guohui Yu,[c] Xuemei Chen,[d] Huishan Wang,[a] Xiaofan Zhou,[a] Lisheng Liao,[a] Lianhui Zhang[a,c]

[a]Guangdong Laboratory of Microbial Signals and Disease Control, Integrative Microbiology Research Centre, South China Agricultural University, Guangzhou, China
[b]Ministry of Education Key Laboratory for Ecology of Tropical Islands, Key Laboratory of Tropical Animal and Plant Ecology of Hainan Province, College of Life Sciences, Hainan Normal University, Haikou, China
[c]Institute of Plant Health, Zhongkai University of Agriculture and Engineering, Guangzhou, China
[d]College of Forestry and Landscape Architecture, South China Agricultural University, Guangzhou, China

Jinli Yan and Peng Li contributed equally to this article. Author order was determined by the corresponding author after negotiation.

ABSTRACT Quorum sensing (QS) is a widely conserved bacterial regulatory mechanism that relies on production and perception of autoinducing chemical signals to coordinate diverse cooperative activities, such as virulence, exoenzyme secretion, and biofilm formation. In *Ralstonia solanacearum*, a phytopathogen causing severe bacterial wilt diseases in many plant species, previous studies identified the PhcBSR QS system, which plays a key role in regulation of its physiology and virulence. In this study, we found that *R. solanacearum* strain EP1 contains the genes encoding uncharacterized LuxI/LuxR (LuxI/R) QS homologues (RasI/RasR [designated RasI/R here]). To determine the roles of the RasI/R system in strain EP1, we constructed a specific reporter for the signals catalyzed by RasI. Chromatography separation and structural analysis showed that RasI synthesized primarily *N*-(3-hydroxydodecanoyl)-homoserine lactone (3-OH-C12-HSL). In addition, we showed that the transcriptional expression of *rasI* is regulated by RasR in response to 3-OH-C12-HSL. Phenotype analysis unveiled that the RasI/R system plays a critical role in modulation of cellulase production, motility, biofilm formation, oxidative stress response, and virulence of *R. solanacearum* EP1. We then further characterized this system by determining the RasI/R regulon using transcriptome sequencing (RNA-seq) analysis, which showed that this newly identified QS system regulates the transcriptional expression of over 154 genes associated with bacterial physiology and pathogenic properties. Taken together, the findings from this study present an essential new QS system in regulation of *R. solanacearum* physiology and virulence and provide new insight into the complicated regulatory mechanisms and networks in this important plant pathogen.

IMPORTANCE Quorum sensing (QS) is a key regulator of virulence factors in many plant-pathogenic bacteria. Previous studies unveiled two QS systems (i.e., PhcBSR and SolI/R) in several *R. solanacearum* strains. The PhcBSR QS system is known for its key roles in regulation of bacterial virulence, and the LuxI/LuxR (SolI/R) QS system appears dispensable for pathogenicity in a number of *R. solanacearum* strains. In this study, a new functional QS system (i.e., RasI/R) was identified and characterized in *R. solanacearum* strain EP1 isolated from infected eggplants. Phenotype analyses showed that the RasI/R system plays an important role in regulation of a range of biological activities associated with bacterial virulence. This QS system produces and responds to the QS signal 3-OH-C12-HSL and hence regulates critical bacterial abilities in survival and infection. To date, multiple QS signaling circuits in *R. solanacearum* strains are still not well understood. Our findings from this study provide new insight into the complicated QS regulatory networks that govern the physiology and

Editor Hideaki Nojiri, The University of Tokyo

Address correspondence to Lisheng Liao, lishengliao@outlook.com, or Lianhui Zhang, lhzhang01@scau.edu.cn.

The authors declare no conflict of interest.

Received 21 February 2022
Accepted 30 June 2022
Published 25 July 2022

virulence of *R. solanacearum* and present a valid target and clues for the control and prevention of bacterial wilt diseases.

KEYWORDS cell-cell communication, signaling mechanism, pathogenesis, bacterial wilt

Ralstonia solanacearum is the causal agent of bacterial wilt and infects over 200 plant species in 50 families throughout tropical and warm temperate regions all over the world (1). Its hosts include many agronomically important crops, such as eggplants, tomatoes, potatoes, and tobacco (2); thus, the pathogen poses a great threat to agricultural industry (3). As a soilborne and waterborne pathogen with superb abilities to adapt to environmental changes, *R. solanacearum* can survive and disperse for years in infected fields (4). Once encountering susceptible plants, *R. solanacearum* locates plant hosts by sensing and chemotaxis toward root exudates by using flagellar motility (5) and then infecting plants through wounds or at the points of emergence of lateral roots. The common sign of the disease is the presence of bacterial cells massively colonizing the plant xylem vessels, resulting in vascular dysfunction and severe wilt as the primary symptom (1). The plant cell wall-degrading enzymes (PCWDEs), twitching and swimming motility, extracellular polysaccharide (EPS), and dozens of type III effectors are needed for the full bacterial virulence (6, 7).

Quorum sensing (QS) is a widely conserved bacterial cell-to-cell communication mechanism that coordinates various bacterial community activities, including bioluminescence, extracellular enzyme production, motility, biofilm formation, and virulence (8–11). By secreting the diffusible signals and sensing their surrounding concentrations, bacterial cells can recognize their populations and thus regulate the expression of a set of target genes in a population-density-dependent manner. A range of QS systems have been unveiled over the years, and among them, the LuxIR system represents the most characterized of the QS systems, with over 100 species of *Proteobacteria* using small diffusible *N*-acyl-homoserine lactones (AHLs) as QS signals. In this system, LuxI is the AHL synthase and LuxR is the AHL-dependent transcription factor (11, 12). LuxR interacts with the cognate AHL signal to form the LuxR-AHL complexes, which then bind at a specific DNA sequence called the *lux* box in the target promoters to modulate gene expression (13). Interestingly, a bacterial species may evolve more than one set of QS systems to modulate its physiology and virulence (14). For example, *Pseudomonas aeruginosa* uses at least four types of QS signaling systems, which constitute a multilayer hierarchy of a regulatory network (15, 16), and *Burkholderia thailandensis* has three complete LuxR/LuxI circuits (17). The environmental selective pressures that result in multiple QS signaling circuits in bacteria are not well understood, although it has been suggested that the different properties of QS signaling might provide specific benefits in different ecological niches (18).

In *R. solanacearum*, two QS systems have been characterized, including a LuxIR homologous system known as SolIR and the PhcBSR system presented only in *R. solanacearum* species. The SolIR QS system was initially identified in *R. solanacearum* GMI1000, in which SolI synthesizes C6- and C8-homoserine lactone (HSL) signals. However, this QS system appears dispensable for virulence as deletion mutation of either SolI or SolR did not seem to alter its pathogenic potential (19). The PhcBSR QS system consists of the methyltransferase PhcB, which synthesizes the QS signal (*R*)-methyl 3-hydroxypalmitate (3-OH PAME) or (*R*)-methyl 3-hydroxymyristate (3-OH MAME) (20–22), and the two-component system PhcS and PhcR, which detects and responds to the QS signal molecules mentioned above. When the signal molecule reaches a threshold level, PhcS/PhcR phosphorylation will be activated, which subsequently elevates the levels of functional PhcA. The activated master regulator PhcA initiates the production of a range of virulence factors, such as exopolysaccharide (EPS) and plant cell wall-degrading enzymes (PCWDEs) required for late-stage infection (23), and the type III secretion system (T3SS) required for early-stage infection (19, 21, 24–26).

In the genome analysis of *R. solanacearum* EP1, which is a virulent strain isolated from severely infected eggplants (*Solanum melongena* L) in Guangdong, China, we found that the pathogen contains another set of *luxI*/*luxR* homologues in addition to previously reported *solI*/*solR*. To explore its potential roles, in the present study, we performed a functional analysis of this new QS system, RasI/RasR (designated RasI/R here), in strain EP1. We first constructed an RasI signal-specific reporter to facilitate signal purification and characterization. We showed that RasI is responsible for the synthesis of primary signal *N*-(3-hydroxydodecanoyl)-HSL (3-OH-C12-HSL) and a small quantity of *N*-(3-hydroxytetradecanoyl)-HSL (3-OH-C14-HSL) in *R. solanacearum* strain EP1. Genetic and biochemical analyses validated that RasR is the cognate receptor responding to 3-OH-C12-HSL and 3-OH-C14-HSL signals in modulating the expression of target genes, including the QS signal synthase gene *rasI*. Phenotype analysis demonstrated that the RasI/R QS system plays a key role in modulating production of plant cell wall-degrading enzymes (PCWDEs), twitching and swimming motility, biofilm formation, and oxidative stress response, which are essential for the full virulence of *R. solanacearum* strain EP1 on host plants.

RESULTS

Bioinformatic analysis of the *lux* QS gene homologs in *R. solanacearum* EP1. In our effort to elucidate the regulatory mechanisms that govern the virulence of *R. solanacearum* strain EP1, which was a dominant bacterial wilt pathogen in Guangdong Province, China, we analyzed the recently sequenced genome of *R. solanacearum* strain EP1 (GenBank accession no: CP015115.1 and CP015116.1). In this process, two previously unreported *luxI*/*luxR* homologous genes (*AC251_22465* and *AC251_22460*; here designated *rasI* and *rasR*, respectively) caught our attention. These two genes are located on the megaplasmid, while the genes coding for SolR and SolI, which were initially identified in in *R. solanacearum* strain GMI1000, are located on the chromosomal DNA. Significantly, the *rasI*/*rasR* homologues were conserved in the *R. solanacearum* strains of phylotype I, III and IV, while not detected in the strains of phylotype II. The amino acid sequence of RasI is identical to that of *R. solanacearum* strain GMI1000 (phylotype I, France), and shares about 98.9%, 98.9%, 96.2%, and 84.78% identity, respectively, with those of its counterparts in four other *R. solanacearum* strains, including strains FQY_4 (phylotype I, China), SD54 (phylotype I, China), CMR15 (phylotype III, Cameroon), and PSI07 (phylotype IV, Indonesia). Similarly, RasR of strain EP1 shares about 100%, 100%, 100%, 97.48%, and 89.08% sequence homologies at the peptide level with its homologs in strains GMI1000, FQY_4, SD54, CMR15, and PSI07, respectively. In contrast, RasI/RasR only shares about 34.8%/37.4% identities with the SolI/SolR of *R. solanacearum* strain EP1 and 28.4%/24.7% identities with the LuxI/LuxR of *Vibrio fischeri*. RasI was found within the family of genes encoding putative acyl-acyl carrier protein (ACP)-dependent AHL synthases by KEGG Orthology (KO) classification (27) (Fig. 1A). Phylogenetic analysis showed that its most close homologue is MbaI (51.63% similarity) from *Methylobacter tundripaludum* (Fig. 1A). MbaI is responsible for biosynthesis of the QS signal *N*-3-hydroxydecanoyl-L-homoserine lactone (3-OH-C10-HSL) and a small quantity of *N*-3-hydroxydodecanoyl-L-homoserine lactone (3-OH-C12-HSL) (28), which is involved in regulating the biosynthesis of the secondary metabolite tundrenone (29).

Specific bioassay system for RasI signals. To purify and identify the signal(s) produced by RasI, we decided to construct a RasI signal-specific reporter. Sequence alignment unveiled that the *rasI* promoter contains a conserved LuxR binding motif (Fig. 1B), suggesting that transcriptional expression of *rasI* could be autoinduced by the RasI signal. We hence generated a RasR-P*rasI*-mCherry reporter construct (pYJL01) by fusing the *rasI* promoter with the open reading frame (ORF) of the mCherry gene, which together with the RasR coding sequence were cloned in the expression vector pBBPgdh and introduced in the non-QS heterologous host *Pseudomonas putida* F1 to produce the reporter strain YJL01 (see Fig. S1 in the supplemental material). This construct was generated on the assumption that the AHL synthase gene *rasI* is controlled in a QS

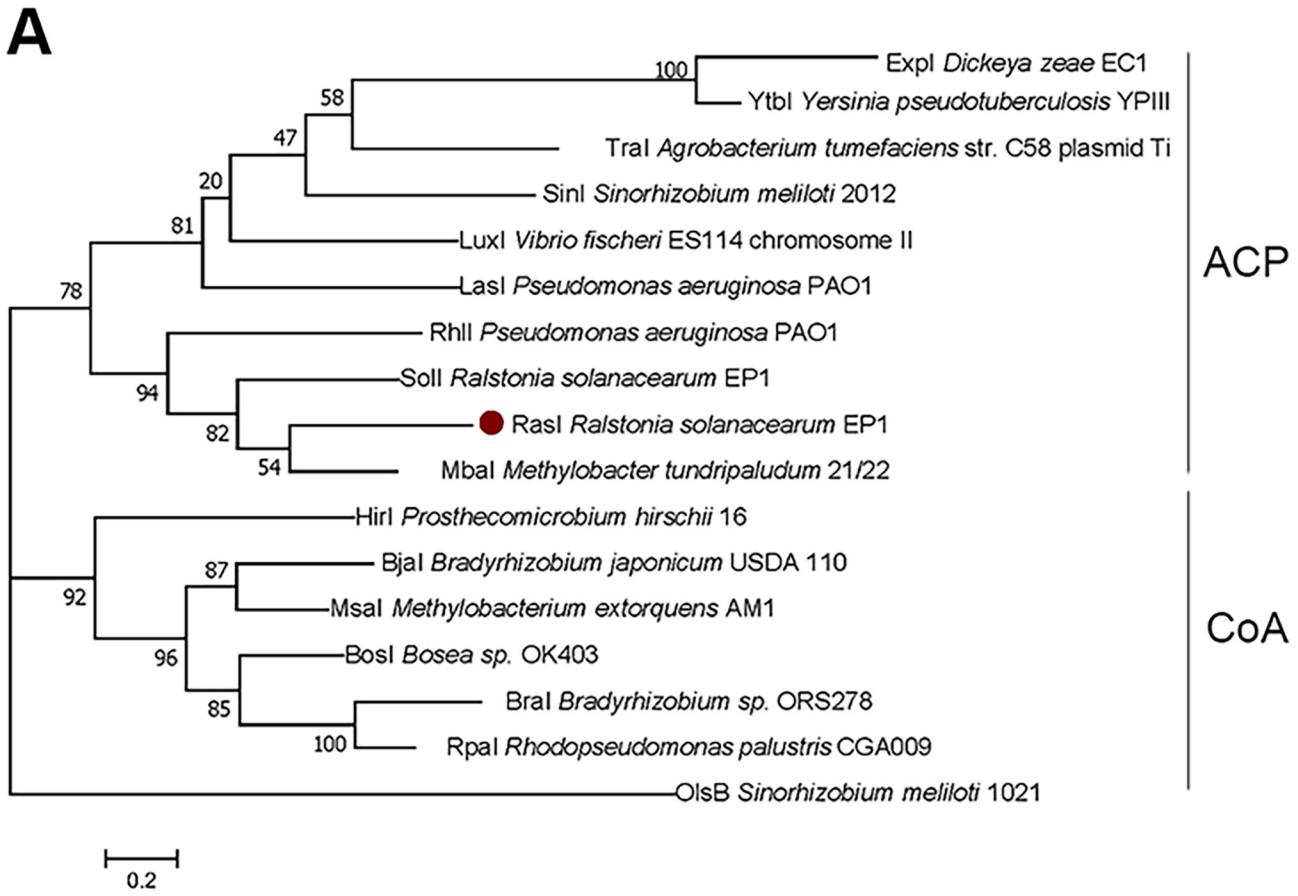

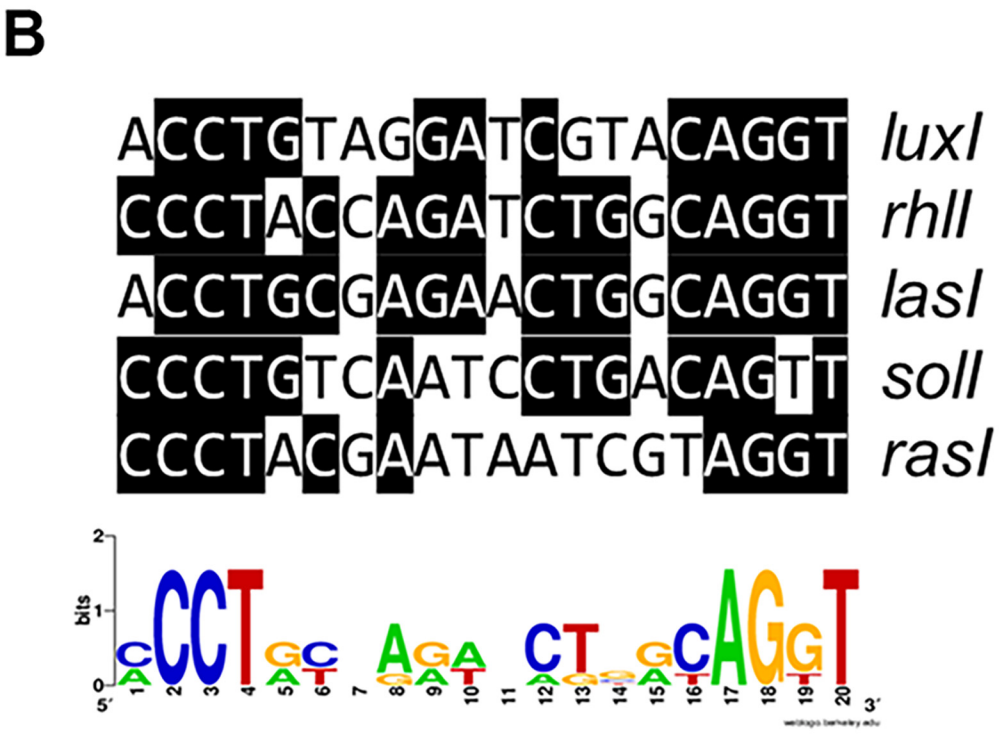

FIG 1 RasI sequence and promoter analysis. (A) Phylogenetic tree of LuxI family members in selected *Proteobacteria*. The phylogenetic tree was constructed using the maximum likelihood method derived from MEGA 7.0 software, and 1,000 bootstrap replicates were included in a heuristic

(Continued on next page)

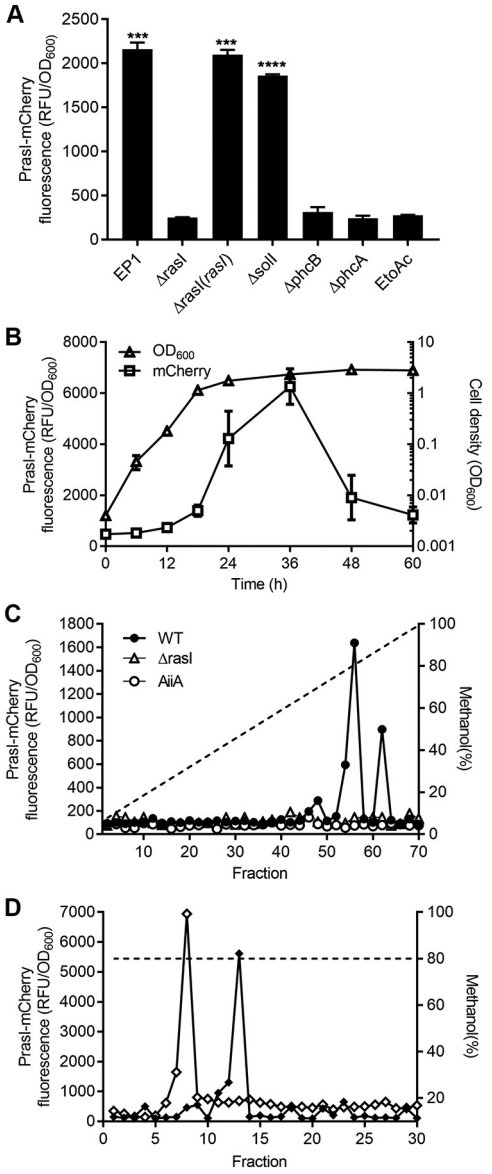

FIG 2 Detection and purification of *R. solanacearum* RasI signals. (A) Detection of AHL signals produced by strain EP1 and its derivatives by reporter YJL01, with ethyl acetate (EtoAc) as a negative control. Error bars the represent standard deviation (SD) of values from three replicates. (B) Growth curve of strain EP1 and the RasI signal accumulation pattern. Error bars represent SD from three replicates. (C) Gradient HPLC profiles of AHLs synthesized by *R. solanacearum* EP1 (●), the *rasI* mutant (△), or EP1 expressing AiiA lactonase (○). The dashed line shows the methanol gradient. (D) Isocratic HPLC profiles of the AHL signals from strain EP1. The dashed line shows the value for 80% methanol. Statistical significance: ***, $P < 0.001$; ****, $P < 0.0001$.

way in which the AHL signal production is activated by the signal-bound LuxR-type receptor RasR (i.e., expression of the P*rasI*-mCherry fusion gene depends upon the presence of RasR and its cognate AHL signal). Bioassay results showed that the resultant reporter strain YJL01 produced a strong fluorescence in response to the culture extracts of *R. solanacearum* strain EP1 (Fig. 2A), validating the feasibility of using this reporter strain to detect the AHL signals produced by strain EP1.

FIG 1 Legend (Continued)

search with a random tree and the tree bisection-reconnection branch-swapping algorithm. The signal synthases RasI is highlighted in a solid red dot. ACP (acyl carrier protein) or CoA (coenzyme A) represents the substrate preference for acyl-HSL synthases. (B) Sequence alignment of the putative RasR-binding site with inverted repeats found in promoter regions of *luxI*-type gene family members from *V. fischeri* ES114 (*luxI*), *P. aeruginosa* PAO1 (*rhlI* and *lasI*), *R. solanacearum* (*solI*). The sequence logo was constructed using WebLogo (http://weblogo.berkeley.edu/).

To identify the RasI-produced AHL signal and eliminate the influence of QS signals produced by SolI, we constructed the *solI* and *rasI* deletion mutants and the *rasI* complemented strain, respectively, in the genetic background of *R. solanacearum* strain EP1. We found that the reporter strain YJL01 could be activated by the ethyl acetate extracts of the cell-free supernatants of strain EP1, the *solI* deletion mutant, and the *rasI* complemented strain (Fig. 2A). In contrast, the signal response was not found in the extracts from the cultures of the *rasI* deletion mutant (Fig. 2A). Thus, these results suggest that the reporter YJL01 is specific to and should be useful for detection of the RasI signal(s) during purification.

To facilitate signal purification, we determined the time course of strain EP1 growth and the pattern of RasI signal accumulation in culture supernatants using the reporter YJL01. The results showed that strain EP1 reached the stationary phase at about 24 h postinoculation, and the accumulation of RasI signal in culture fluid lagged behind the increase of cell density in the early part of growth and then accelerated (Fig. 2B), which is consistent with the positive autoregulation pattern of AHL production. Notably, the signal level reached the maximum at 36 h postinoculation and then decreased rapidly (Fig. 2B).

Purification and identification of RasI signals. To purify the signal molecules synthesized by RasI, the acidified ethyl acetate was used to extract the cell-free supernatants of strain EP1. The signal activity was mainly found in the organic phase, which was then evaporated and dissolved in methanol. The methanol solution was diluted accordingly and fractionated by C_{18} reverse-phase high-performance liquid chromatography (RP HPLC) with a 10 to 100% methanol gradient. Each fraction was assayed using the RasI signal reporter strain YJL01 (Fig. 2C). The majority of signal activity was found in fractions 56 and 62. As a control, the RasI signal activity was not present in the supernatant extract from the Δ*rasI* mutant. Similarly, the RasI signal activity was also not found in the supernatant extract from strain EP1, adding AiiA (AHL lactonase), which hydrolyzes the homoserine lactone ring of AHL family signals (30, 31). The finding agrees with the bioinformatics prediction that the RasI signals are the members of AHL family molecules.

The active fractions from gradient HPLC separation were further fractionated by isocratic HPLC with 80% methanol (Fig. 2D). Under this HPLC elution condition, the RasI signal activity was found in two fractions (i.e., fractions 8 and 13) (Fig. 2D), suggesting that at least two AHL molecules are produced by RasI in strain EP1. To determine the chemical structures of the purified AHL molecules, we scanned and analyzed the two purified fractions by high-resolution liquid chromatography-tandem mass spectrometry (LC-MS/MS). The results showed that the fractions 8 and 13 produced parent ions, $[M+H]^+$, of 300.2165 *m/z* and 328.2483 *m/z*, respectively. Both parent ions were accompanied with an obvious daughter ion, $[M+H]^+ = 102$ (Fig. S2), which is the common characteristic of the homoserine lactone fragment of AHLs (32). The molecular masses of the two fractions are consistent with the molecular formula of *N*-(3-hydroxydodecanoyl)-HSL (3-OH-C12-HSL) and *N*-(3-hydroxytetradecanoyl)-HSL (3-OH-C14-HSL) (Fig. 3A and C). The HPLC retention time and mass spectra (Fig. S2) of these purified compounds were indistinguishable from those of the corresponding commercial standards (Fig. 3B and D). Taken together, these findings demonstrate that two QS signals synthesized by the RasI enzyme in *R. solanacearum* strain EP1 are 3-OH-C12-HSL and 3-OH-C14-HSL (Fig. 3E and F).

To determine the biological activity of these AHL signals, we compared their signaling activities using the reporter strain YJL01. The results showed that the reporter could respond to both AHL signals, but 3-OH-C12-HSL was more potent than 3-OH-C14-HSL, especially at the lower end of the concentration ranges (Fig. 4A). Notably, at the final concentration of 10 nM, the signaling activity of 3-OH-C12-HSL was about 4-fold higher than that of 3-OH-C14-HSL (Fig. 4A). These results, together with those of Fig. 2, suggest that the RasI/R QS system of strain EP1 produces and responds primarily to the AHL family signal 3-OH-C12-HSL.

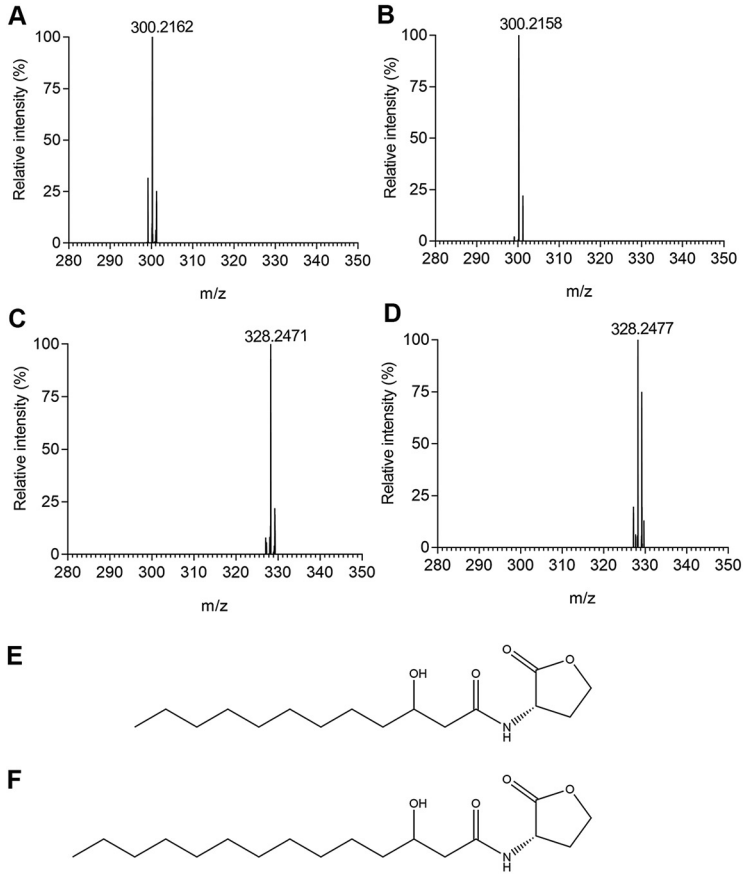

FIG 3 Mass spectrometry characterization of the AHL signals synthesized by RasI. (A and C) Mass spectrum showing the parental ions of fractions 8 (A) and 13 (C) shown in Fig. 2D. (B and D) Mass spectrum showing the parental ions of chemically synthesized 3-OH-C12-HSL (B) and 3-OH-C14-HSL (D). (E and F) Chemical structures of 3-OH-C12-HSL (E) and 3-OH-C14-HSL (F).

To quantify the 3-OH-C12-HSL signal level in *R. solanacearum* strain EP1, we scanned it in the supernatant of wild-type (WT) EP1 culture over the course of bacterial growth. Rapid increase of 3-OH-C12-HSL signal level occurred at the bacterial exponential growth phase (optical density at 600 nm [OD_{600}] of about 0.1 to 1.0), and the maximum accumulation of 3-OH-C12-HSL was up to approximately 500 nM at the stationary phase (Fig. 4B). We then determined the specificity of RasR in response to other AHL family signals by screening nine different AHLs with fatty acyl groups ranging from 4 to 14 carbons. The results showed that at the final concentration of 100 nM, the best signal in activation of the RasR-P*rasI-mCherry* reporter system was 3-OH-C12-HSL, followed by 3-OH-C14-HSL and 3-OH-C10-HSL (Fig. 4C). The reporter could hardly respond to C4-HSL, C6-HSL, C8-HSL, C10-HSL, 3-oxo-C6-HSL, 3-oxo-C8-HSL, 3-oxo-C12-HSL, or 3-OH-C8-HSL (Fig. 4C), even at a high concentration (1 μM) (data not shown). Obviously, the signal receptor RasR tends to respond to long-chain 3-hydroxyl AHLs.

The RasI/R QS system controls a range of biological functions. To determine the biological functions regulated by the RasI/R QS system, we constructed *rasI*, *rasR*, *solI*, *solR*, *phcA*, and *phcB* deletion mutants, using WT EP1 as the parental strain, as well as the corresponding *rasI* and *rasR* complemented strains. Phenotype analysis showed that the deletion of *phcA*, *phcB*, *rasI*, or *rasR* caused a substantial reduction in the cellulase (CEL) activity, while deletion of *solI* and *solR* did not seem to influence CEL activity (Fig. 5A). On a semisolid motility agar assay, the Δ*rasI* and Δ*rasR* mutants showed significantly weakened swimming ability compared with the WT strain (Fig. 5B). Notably, the Δ*phcA* and Δ*phcB* mutants were more hypermotile than the wild-type EP1 strain (Fig. 5B). Under the microscope, the *R. solanacearum* EP1 wild type and the other

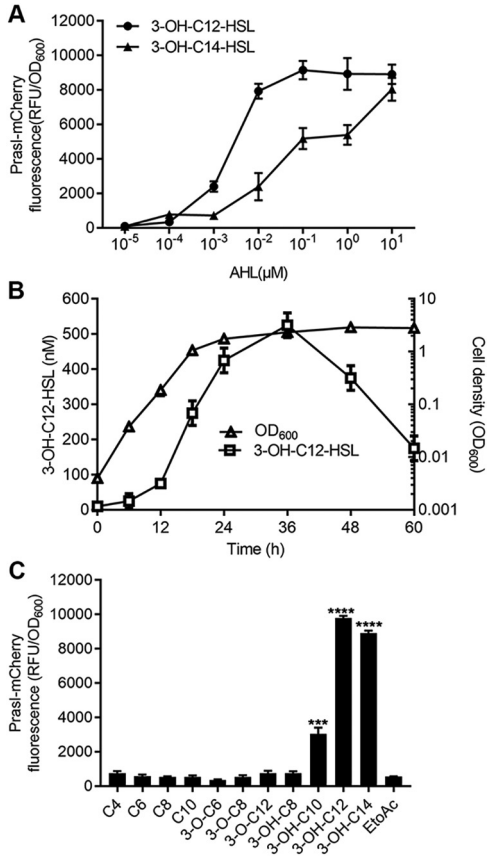

FIG 4 *R. solanacearum* EP1 produces primarily 3-OH-C12-HSL and responds to the long-chain 3-hydroxyl AHLs. (A) Dose response of the YJL01 reporter strain to 3-OH-C12-HSL (●) and 3-OH-C14-HSL (▲); (B) 3-OH-C12-HSL accumulation (□) during *R. solanacearum* growth (△); (C) relative activity of various AHLs in induction of the reporter strain YJL01. Each AHL signal was assayed at the final concentration of 100 nM. Error bars represent SD from three replicates. Statistical significance: ***, $P < 0.001$; ****, $P < 0.0001$.

mutants appeared to produce motile rafts of cells with clear striates in the colony edge, as previously reported (33), while the Δ*rasI* and Δ*rasR* mutants were deficient for twitching motility (Fig. S3). Furthermore, we found that deletion of *rasI* and *rasR* caused much increased biofilm formation on the CTG liquid medium compared with the WT EP1 (Fig. 5C). In contrast, deletion of *phcB* and *phcA* caused only a slight increase in biofilm formation, and deletion of *solI* and *solR* did not apparently affect biofilm production compared to that of WT EP1 (Fig. 5C). Expression of the corresponding WT *rasI* gene in Δ*rasI*(*rasI*) complemented strains and complementation of the Δ*rasR* mutant with WT *rasR* rescued the changed phenotypes to the wild-type levels (Fig. 5A to C), validating the key role of RasI signal and RasR regulatory protein in regulation of these virulence-related traits.

Deletion mutation of RasI/R QS system significantly attenuates bacterial virulence. In the virulence assay, eggplants were inoculated with WT strain EP1 and its derivatives using the naturalistic soil soak inoculation method (34, 35). The plants inoculated with strain EP1 and the Δ*solI* and Δ*solR* mutants displayed wilt symptoms 3 days after inoculation and were eventually killed within 10 days (Fig. 5H; Fig. S4C). In contrast, the Δ*rasI*, Δ*rasR*, Δ*phcA*, and Δ*phcB* mutants failed to cause any death of eggplant plants under the same inoculation conditions, even at 20 days postinoculation (dpi) (Fig. 5H; and Fig. S4A, B, and D). The Δ*rasI*(*rasI*) and Δ*rasR*(*rasR*) complemented strains became fully virulent, similar to the WT strain EP1 (Fig. 5H; Fig. S4A and B). Semiquantitative analysis showed that virulence of *rasI*, *rasR*, *phcB*, and *phcA* deletion mutants was significantly attenuated compared with that of the wild-type strain, while

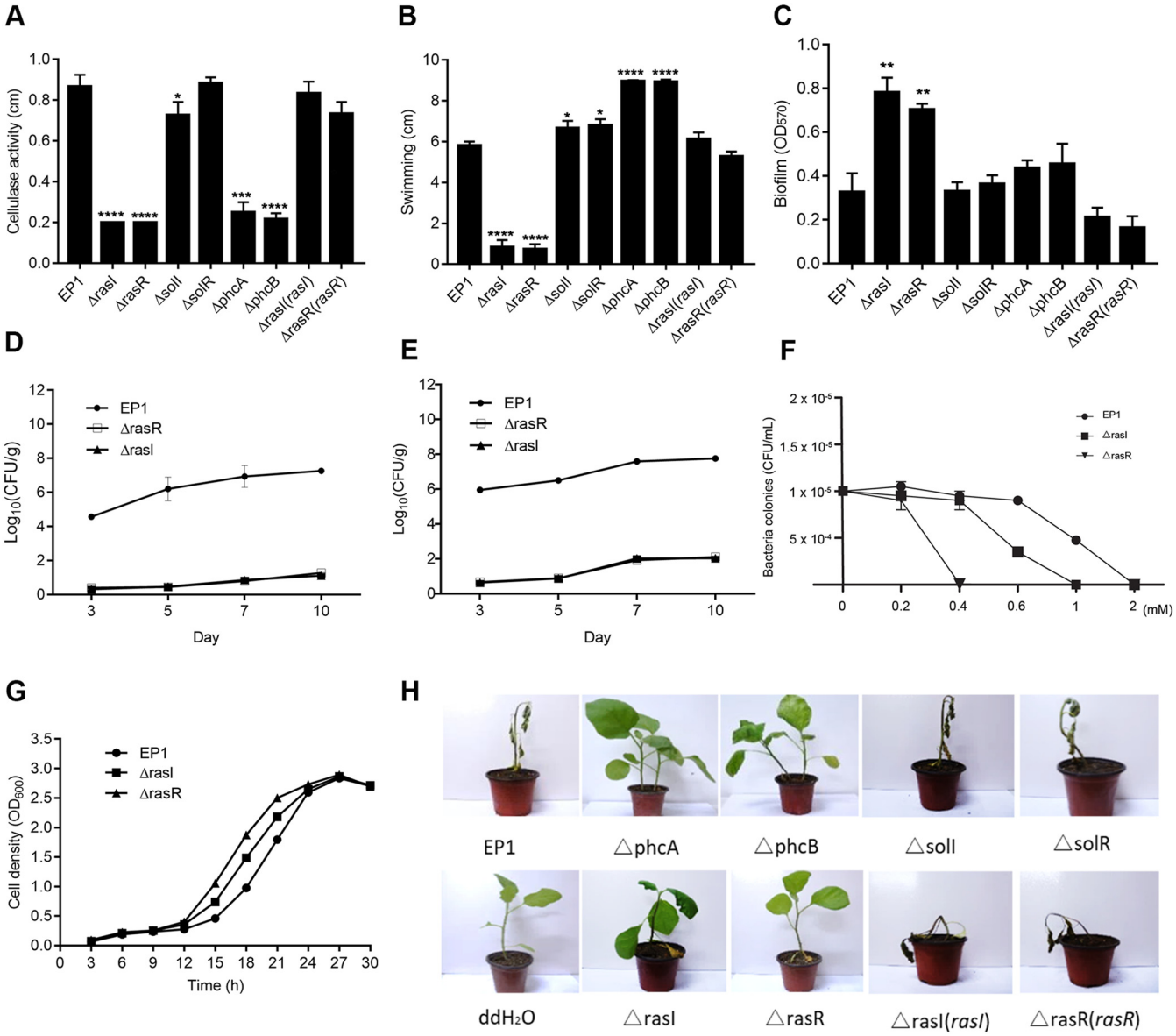

FIG 5 Phenotype analyses of *R. solanacearum* EP1 and derivatives. (A) Cellulase activity; (B) swimming motility; (C) biofilm formation; (D) survival around the inoculation point; (E) systemic infection assay of *R. solanacearum* EP1 and mutants; (F) effect of hydrogen peroxide on bacterial growth; (G) growth curves of *R. solanacearum* EP1 and mutants in CTG medium; (H) plant virulence assay. All of the experiments were repeated at least three times with triplicate bacterial samples or 10 plants per treatment. The data shown are the mean ± SD from three replicates. Statistical significance: *, $P < 0.01$; **, $P < 0.05$; ***, $P < 0.001$; ****, $P < 0.0001$.

the *solI* and *solR* deletion mutants and the Δ*rasI*(*rasI*) and Δ*rasR*(*rasR*) complemented strains showed a similar level of virulence to wild type EP1 (Fig. S4). These results validated the essential role of the RasI/R QS system in regulation of the bacterial pathogenicity.

To determine whether the RasI/R QS system contributes to the systemic infection of *R. solanacearum* in plants, we calculated the bacterial CFU in plant stem or root tissues at different time points following root cutting and soil soaking inoculation. The results showed that the bacterial cells of wild-type EP1 spread rapidly from roots to stem tissues, whereas the numbers of cells of the Δ*rasI* and Δ*rasR* mutants in stem or root tissues were much lower, particularly during the first 7 days postinoculation (Fig. 5D and E). The above findings indicate that the systemic infection abilities and survival around inoculation point of the *rasI/R* mutants were much weakened, which are highly consistent with the results of the virulence assay.

The RasI/R system is involved in regulation of bacterial resistance to oxidative stress. In the process of bacterial infection, pathogenic invaders have to overcome various host defense mechanisms for survival and proliferation. Given that the bacterial virulence and systemic infection ability were much attenuated by deletion mutation of the RasI/R system (Fig. 5E and H), we were curious whether the mutation of this QS system might also affect the pathogen's ability to counteract the defense stresses from host plants. Plant-generated reactive oxygen species (ROS), which act as part of the primary defense responses to pathogenic invasions, are one of the challenges that bacterial invaders commonly encounter during infection. To examine this possibility, we conducted the bacterial survival assay against hydrogen peroxide (H_2O_2), which is the major ROS of the host oxidative burst at the early stage of pathogenic infection. The bacterial cells of strain EP1 and its Δ*rasI* and Δ*rasR* derivatives were cultured in CTG medium, and the fresh bacterial cells after 24 h of culture were taken for the survival assay against H_2O_2. The results showed that three strains grew at a similar rate in CTG medium, though the Δ*rasI* and Δ*rasR* mutants grew slightly faster than WT EP1 (Fig. 5G). The Δ*rasI* mutant was not able to survive at an H_2O_2 concentration higher than 1 mM, and the Δ*rasR* mutant was unable to cope with 0.4 mM H_2O_2, whereas the WT strain EP1 was killed by H_2O_2 only at a much higher concentration—about 2 mM (Fig. 5F).

The RasI/R QS system modulates the expression of multiple genes in *R. solanacearum* EP1. To unveil the regulatory spectrum of the RasI/R QS system, we used transcriptome sequencing (RNA-seq) to compare the genomic transcriptional profiles of the WT strain EP1 and the *rasI* and *rasR* deletion mutants. The analysis identified 228 genes regulated by RasR (21 upregulated and 207 downregulated), defined as more than a 1.5-fold change in expression level by comparing the Δ*rasR* mutant with the WT EP1 (Table S1). Similarly, we found that a total of 223 genes (44 upregulated and 178 downregulated) were regulated by RasI (Table S2). Notably, 154 genes were coregulated by RasR and RasI, which constitutes the RasI/R regulon (Table 1 and Fig. S5C). Thus, among the RasR-regulated genes, about 69% of them were also presented in the RasI regulon, and these genes are associated with a range of biological functions, including transportation, regulation, stress resistance and detoxification, pathogenicity, flagellum synthesis, and fatty acid metabolism (Table 1). Similar signal-dependent, but receptor-independent QS-regulated genes have also been reported previously in the Las and Rhl systems of *P. aeruginosa*, respectively (36, 37). To validate the RNA-seq results, 10 genes were arbitrarily selected for quantitative reverse transcription-PCR (qRT-PCR) analysis (Fig. S5A and B), including *AC251_22465*, encoding an *N*-acylhomoserine lactone synthase, RasI, *AC251_00730*, encoding transcriptional activator protein SolR, *AC251_00725*, encoding fucose-binding lectin, *AC251_19280*, encoding cellulase, *AC251_23955*, encoding type II/IV secretion system protein CpaF, *AC251_19340*, encoding SAM-dependent methyltransferase, *AC251_17135*, encoding a universal stress protein, *AC251_23985*, encoding a type IVb pilin, *AC251_22035*, encoding an AraC family transcriptional regulator, and *AC251_25945*, encoding an isopenicillin synthase (Table S3). The qRT-PCR data of the Δ*rasI* and Δ*rasR* mutants were highly consistent, and the results validated the findings of RNA-seq analysis (Fig. S5A and B). Taken together, the above results indicate that the RasI/R QS system plays an important role in regulation of the bacterial physiology and virulence by modulating the transcriptional expression of a large set of corresponding genes.

DISCUSSION

In this study, a new functional QS system (i.e., RasI/R) was identified and characterized in *R. solanacearum* strain EP1 isolated from infected eggplants (38). Phenotype analyses showed that the RasI/R system plays a key role in regulation of a range of biological activities associated with the bacterial virulence, including cellulase production (Fig. 5A), swimming motility (Fig. 5B), twitching motility (see Fig. S3 in the supplemental material), biofilm formation (Fig. 5C), and oxidative stress response (Fig. 5F). RNA-seq analysis showed that RasR and RasI regulate the transcriptional expression of 228 and 223 genes, respectively (Tables S2 and S3 and Fig. S5C). A subset of genes selected

TABLE 1 Functional groups of the genes co-regulated by RasR and RasI[a]

Gene family	Gene name or ID	Log2Fold changes RasR vs WT (P_{adj}[b] < 0.05)
Membrane component and transporter		
Membrane protein	*ompW,* AC251_02870, AC251_04210, AC251_04770, AC251_06130, AC251_08165, AC251_13900, AC251_23345, AC251_24890, AC251_24895, AC251_25935, AC251_03860 AC251_00725	−1.89–−3.69
ABC transporters	AC251_23810	−2.20
Transporter	AC251_07410, AC251_16330, AC251_23670, AC251_13370	−1.75–−2.47
Regulator		
Transcriptional regulator	*solR,* AC251_00235, AC251_09675, AC251_13820, AC251_15330, AC251_20605, AC251_22035, AC251_22575, AC251_23470	−1.91–−2.60
Signal synthesis	*rasI,* AC251_06640, AC251_25845	−1.56–−2.09
Stress resistance and detoxification		
Stress resistance	AC251_17135, AC251_18370	−3.20–−3.54
Detoxification	AC251_14105	−1.80
Pathogenicity		
Type III secretion	AC251_22915, AC251_23955, AC251_23965	−1.68–−3.46
Virulence	*mprA,* AC251_19195, AC251_19280, AC251_19825, AC251_19835	−1.68–−3.46
Protein metabolism		
Protein biosynthesis and degradation	AC251_01470, AC251_16810, AC251_21480	−1.82–−4.04
Protein export		
Others	AC251_14960, AC251_16375, AC251_21190, AC251_23940	−1.64–−4.07
Flagellum synthesis, motility and chemotaxis		
Pili	AC251_23970, AC251_23975, AC251_23980, AC251_23985	−1.85–−3.25
Flagellar	AC251_25380, AC251_25385	−2.28–−2.45
TCA cycle and fatty acid metabolism		
Metabolism	AC251_16945, AC251_19335, AC251_19340	−1.68–−4.33
Fatty acid synthesis	AC251_07405	−2.71
Microbial metabolism		
Phosphorylation	AC251_11000, AC251_16920, AC251_18470, AC251_23850	−1.84–−3.36
Biodegradation	AC251_08405, AC251_08410, AC251_13835, AC251_17060, AC251_17865, AC251_18450, AC251_19840, AC251_22735, AC251_23840,	−2.04–−6.55
Small molecule metabolism	AC251_02875, AC251_08175, AC251_12535, AC251_13830, AC251_14030, AC251_16360, AC251_23845, AC251_25950, AC251_17795	−2.19–−3.70
Biosynthesis	AC251_21490, AC251_21985, AC251_24430, AC251_24450, AC251_25945	−1.95–−3.55
Cell processes		
Chromosome associated protein	AC251_18440	−3.15
Hypothetical protein	AC251_00610, AC251_00820, AC251_00955, AC251_01460, AC251_01765, AC251_01855, AC251_01995, AC251_02915, AC251_04260, AC251_04315, AC251_05905, AC251_06160, AC251_06550, AC251_06635, AC251_06725, AC251_07010, AC251_08090, AC251_08170, AC251_08190, AC251_08195, AC251_08210, AC251_08580, AC251_08900, AC251_08905, AC251_08910, AC251_09280, AC251_09285, AC251_09290, AC251_09295, AC251_09965, AC251_11895, AC251_13350, AC251_13355, AC251_13360, AC251_13365, AC251_13375, AC251_13895, AC251_15040, AC251_15070, AC251_16365, AC251_16425, AC251_16580, AC251_16860, AC251_16925, AC251_17065, AC251_18280, AC251_18445, AC251_18455, AC251_18460, AC251_18465, AC251_18475, AC251_19110, AC251_19320, AC251_19330, AC251_20475, AC251_20610, AC251_21345, AC251_22045, AC251_22165, AC251_23175, AC251_23540, AC251_23935, AC251_25790	−1.62–−5.94

[a]Functional analysis was according to KEGG and gene annotation. Detailed information is provided in Tables S2, S3.
[b]Padj, adjusted *P* value.

from the RNA-seq results were confirmed by qRT-PCR analysis, indicating the key roles of this newly identified QS system in modulation of the expression of virulence genes. In great agreement with the genetic and biochemical results, the virulence assay showed that deletion mutation of either *rasI* or *rasR* in *R. solanacearum* strain EP1 largely blocked its pathogenicity, survival, and systemic infection on eggplant plants (Fig. 5D, E, and H; Fig. S4). Interestingly, the *rasR* and *rasI* mutants could grow faster at the exponential phase than the wild-type strain EP1 in CTG medium (Fig. 5G), whereas their CFU *in planta* were much lower than those of strain EP1 (Fig. 5D and E). The findings suggest that in addition to the attenuated bacterial motility (Fig. 5B), which is key for bacterial infection and systemic infection, the compromised oxidative stress resistance of these mutants (Fig. 5F) might also be an important factor accounting for their limited survival *in planta* (Fig. 5D).

Comparison of the RasI and RasR regulons identified a common set of 154 genes (Fig. S5C), which could be grouped into at least 7 functional categories, including transportation, regulation, stress resistance and detoxification, pathogenicity, flagellum synthesis, and fatty acid metabolism (Table 1). Numerous studies have demonstrated that the type III secretion system (T3SS) and motility are important virulence factors for early infection and adaption to a changing environment (6, 39, 40). RNA-seq analysis in this study showed that deletion of *rasI* or *rasR* caused downregulation of T3SS protein HrpB4 (Table 1 and data not shown). To our knowledge, the role of HrpB4 has not yet been characterized in *R. solanacearum*, but recent studies in *Xanthomonas campestris* pv. *vesicatoria* and *Xanthomonas citri* subsp. *citri* showed that it is an essential pathogenicity factor playing a key role in promoting docking of the sorting platform to T3SS and thus secretion of T3SS effectors (41, 42). It is plausible that downregulation of *hrpB4* might restrain translocation of T3SS effectors from *R. solanacearum* to the host plant. In *R. solanacearum*, swimming motility is mediated by polar flagella, and the flagellar subunit protein FliC or motor switch protein FliM mutants were nonmotile and showed reduced virulence in tomato (43). Twitching motility is another type of movement used by *R. solanacearum*, which is driven by type IV pilus (TFP) appendages (6). Characterization of several TFP$^-$ mutants of *R. solanacearum* unveiled that pili contribute to natural competence, biofilm formation, and multiple stages of pathogenesis (5, 6). The results of RNA-seq indicate that these motility-related genes were downregulated when the *rasI* or *rasR* gene was deleted (Table 1; Tables S2 and S3 and data not shown). These findings are highly consistent with the results of virulence assay that deletion mutation of the RasI/R QS system abrogated the bacterial systemic infection ability and virulence (Fig. 5E and H; Fig. S4). Thus, the RNA-seq analysis data provided a molecular basis underpinning the critical roles of the RasI/R QS system in modulation of the physiology and virulence of *R. solanacearum* EP1.

R. solanacearum strains collected from different regions of the world are usually remarkably different in various properties, such as host range, pathogenicity, and physiology (2, 44, 45). It has become clear that *R. solanacearum* is a species complex (RSSC) consisting of a heterogeneous group of related but genetically distinct strains (38). Based on the genetic similarities of the internal transcribed spacer region, hypersensitive response and pathogenicity (*hrp*) gene *hrpB*, and endoglucanase, *R. solanacearum* species were grouped into 4 phylotypes (I to IV) (4). In this context, it is interest to note that the genes encoding the RasI/R QS system are present in all the phylotype I strains used in this study (GMI1000, FQY_4, EP1, and YC45, SD54), as well as the phylotype III (CMR15) and phylotype IV (PSI07) strains, but were not discovered in all the sequenced phylotype II strains deposited in the NCBI database. Genome sequence analysis showed that the *rasI/R* genes are located in the megaplasmid, in which many important virulence genes are also located, such as the *hrp* clusters (T3SS), c-di-GMP genes, flagellar genes, and T6SS genes (38, 46). In this regard, it is interesting to note that both the *solI/R* and *phcBSR* QS genes, which are conserved in all the four phylotypes, are located on the chromosome of *R. solanacearum*. These findings suggest that the RasI/R QS system might have coevolved with the other virulence genes in the megaplasmid of RSSC.

Previous studies unveiled two QS systems (i.e., PhcBSR and SolI/R) in several *R. solanacearum* strains. The PhcBSR QS system is known for its key roles in regulation of EPS and cellulase production, T3SS, and bacterial virulence (19–22, 24, 25). Similar to the RasI/R

system, the SolI/R system also produces and responds to AHL family QS signals (i.e., C6-HSL and C8-HSL) (19, 21, 47). However, the SolI/R QS system appears dispensable for pathogenicity and seems to influence the expression of only three genes (i.e., *aidA*, *lecM*, and *aidC*) (1, 19). The *aidA* and *aidC* genes encode proteins that have not yet been functionally characterized, while *lecM* encodes a mannose-fucose binding lectin (21). Consistent with the previous reports, we found that in *R. solanacearum* strain EP1, the PhcBSR QS system is essential for the bacterial virulence, whereas deletion mutation of SolI/R did not seem to affect its pathogenicity on eggplants (Fig. 5H). This suggests that the biological functions of these two QS systems are widely conserved. We also noticed that deletion of *phcB* and *phcA* almost abolished the transcriptional expression of *rasI* and *solI*, whereas deletion of *solI* did not have much of an effect on the transcript level of *rasI* (Fig. 2A; and Fig. S6). In contrast, deletion of either *rasI* or *rasR* almost blocked transcriptional expression of *solI* (Fig. S6). These findings suggest that the three QS systems constitute a hierarchical QS network in *R. solanacearum*, in which PhcBSR controls the expression of RasI/R and the latter regulates the expression of SolI/R.

It is intriguing that the two AHL-type QS systems in *R. solanacearum* evolved in such a way with stringent signal specificity (Fig. 2A), which may be essential for executing different biological functions, respectively, reminiscent of those of the LasI/R and RhlI/R QS systems in *Pseudomonas aeruginosa* (16, 48). However, given that the AHL-type QS systems are widely conserved in prokaryotes, the influence of interspecies communication on bacterial physiology and microbial ecology may deserve attention. The RasI in *R. solanacearum* EP1 synthesizes 3-OH-C12-HSL primarily, and RasR responds to long-chain 3-hydroxyl AHLs, such as 3-OH-C12-HSL, 3-OH-C14-HSL, or 3-OH-C10-HSL, and was sensitive to and responded to 3-OH-C12-HSL and 3-OH-C14-HSL signals at a nanomolar level (Fig. 4). The long-chain 3-hydroxyl AHL signals have also been produced by a few bacterial species and play roles in modulation of various biological activities, including regulation of antibiotic biosynthesis in *Burkholderia thailandensis* (17), secondary metabolite tundrenone production in *Methylobacter tundripaludum* (28), and drug resistance gene expression and affecting biofilm formation and flagellar movement in *Acinetobacter baumannii* (49), biofilm formation and bacterial motility in *Acinetobacter nosocomialis* (50), and nitrogen metabolism in *Nitrosospira briensis* (32). Particularly, *Burkholderiales* and *Methylococcales* have also been identified in enrichments from eggplant soil samples (51, 52), which suggests the possibility of cross talk among these bacterial species in the soil environment surrounding host root systems. Given the key roles of the similar AHL signals in modulation of bacterial pathogenicity and antibiotic production, respectively, in different bacterial species living in the same niche, it would be of significant interest to investigate the impact of this signal-mediated interspecies communication on bacterial wilt epidemiology and on soil microbiome structure.

In summary, this study identified a previously unreported QS system, RasI/R, in *R. solanacearum* strain EP1. This new QS system produces and responds to the QS signals 3-OH-C12-HSL and 3-OH-C14-HSL and hence regulates critical bacterial abilities involved in survival and infection. The findings from this study provide new insight into the complicated regulatory networks that govern the physiology and virulence of *R. solanacearum* and present a valid target and clues for the control and prevention of bacterial wilt diseases.

MATERIALS AND METHODS

Bacterial strains and growth conditions. The plasmids and bacterial strains used in this study are listed in Table 2. *R. solanacearum* strains were grown at 28°C overnight in CTG rich broth (53), which consists of 10.0 g of tryptone, 5.0 g of glucose, and 1.0 g of Casamino Acids per L, or in TZC (CTG agar containing 0.005% of tetrazolium chloride) plates. *P. putida* F1 and RasR-P*rasI*-mCherry reporter strain YJL01 were cultured at 30°C in Luria-Bertani (LB) broth, and *Escherichia coli* strains were cultured at 37°C in LB broth, which consists of 10.0 g of tryptone, 5.0 g of yeast extract, and 10.0 g of NaCl per L. The swimming motility soft agar contains 10.0 g bacteriological peptone, 3.0 g bacteriological yeast extract, 3.0 g bacteriological agar per L. The twitching motility testing agar contains 10.0 g of tryptone, 5.0 g of glucose, 1.0 g of Casamino Acids, and 16 g of bacteriological agar per L. The cellulase activity testing agar contains 1.0 g carboxymethyl ethyl cellulose, 3.8 g sodium phosphate, and 8.0 g agarose per L. Antibiotics were used as needed at the following concentrations: 100 μg/mL ampicillin, 100 mg/L kanamycin, and 15 μg/

TABLE 2 Strains, plasmids and primers used in this study

Strains/plasmids/primers	Characteristics	Source or usage
Strains		
EP1	*R. solanacearum* EP1, wild type strain, Rif^R	(34)
GMI1000	*R. solanacearum* GMI1000, wild type strain, Rif^R	(56)
ΔrasI	The *rasI* gene deletion mutant of strain EP1, Rif^R	This study
ΔrasI (*rasI*)	Complemented strain, ΔrasI expressing *rasI,* Km^R, Rif^R	This study
ΔrasR	The *rasR* gene deletion mutant of strain EP1, Rif^R	This study
ΔrasR(*rasR*)	Complemented strain, ΔrasR expressing *rasR,* Gm^R, Rif^R	This study
ΔsolI	The *solI* gene deletion mutant of strain EP1, Rif^R	This study
ΔsolR	The *solR* gene deletion mutant of strain EP1, Rif^R	This study
ΔphcA	The *phcA* gene deletion mutant of strain EP1, Rif^R	This study
ΔphcB	The *phcB* gene deletion mutant of strain EP1, Rif^R	This study
P. putida F1	*P. putida,* wild type strain	(36)
YJL01	*P. putida* F1 containing AHL reporter construct pYJL01	This study
YJL02	*P. putida* F1 containing AHL reporter construct pYJL02	This study
E. coli DH5α	80dlacZΔM15Δ(lacZYA-argF)U169 recA1 endA1 hsdR 17 supE44 thi-1 gyrA relA1	Transgen
Plasmids		
pK18mobsacB	Suicide and narrow-broad-host vector, Gm^R	This study
pBBR1MCS2/5	Broad-host-range cloning vector, Km^R/Gm^R	This study
pRK2013	Tri-parental mating help plasmid, Km^R	This study
pBBPgdh	Pbbr1MCS-5 with *RPA0944* promoter between KpnI and XhoI sites, Gm^R	(36)
pYJL01	pBBPgdh with *rasR*-P*rasI-mCherry* fusion gene, Gm^R	This study
pYJL02	pBBPgdh with *solR*-P*soll- mCherry* fusion gene, Gm^R	This study
pBBR1MCS2-*rasI*	pBBR1MCS2 with *rasI* and its native promoter, Km^R	This study
pBBR1MCS5-*rasR*	pBBR1MCS5 with *rasR* and its native promoter, Gm^R	This study
Primer		
rasI-1	5′-CGGAATTCTTGCTGAACAACTACCCGC	Deletion of *rasI*
rasI-2	5′-CCATTCGTTTCAGTCAGGCCGACGAATACCTTGTAGCG	
rasI-3	5′-CGCTACAAGGTATTCGTCGGCCTGACTGAAACGAATGG	
rasI-4	5′-CGGGATCCGATTCGCCAATGACATCC	
rasR-1	5′-CGGGATCCGTTATCGAGATGAACATTG	Deletion of *rasR*
rasR-2	5′-CAGCAGATCTTCTTGCCAACAATGTTCATCTCGATAAC	
rasR-3	5′-GTTATCGAGATGAACATTGTTGGCAAGAAGATCTGCTG	
rasR-4	5′-CCAAGCTTACCAGGTCATCTCCGAAC	
phcA-1	5′-TGAACCACGGCACCTACAA	Deletion of *phcA*
phcA-2	5′-AACAGCCGCCTCATCAAATGGCTCAGACAGAAGGTGGA	
phcA-3	5′-TCCACCTTCTGTCTGAGCCATTTGATGAGGCGGCTGTT	
phcA-4	5′-GCAGACCTCAAGAACATCG	
phcB-1	5′-CGGGATCCCTGTTCGGCAAGTACAATCG	Deletion of *phcB*
phcB-2	5′-TTTCCACGGTGTGCGTCCGCTGCAGCGTGATGATGGTG	
phcB-Gen-1	5′-CACCATCATCACGCTGCAGCGGACGCACACCGTGGAAA	
phcB-Gen-2	5′-GAACACGTTGACACCGGTATGGCGGCGTTGTGACAATTT	
phcB-3	5′-AAATTGTCACAACGCCGCCATACCGGTGTCAACGTGTTC	
phcB-4	5′-GCGTCGACCTCGGTGAGGCTGTGGTTGAT	
rasI-F	5′-CCAAGCTTTGTCTTGCGCCGCGTTTCTC	Complementary *rasI*
rasI-R	5′-CGGGATCCCCATTCGTTTCAGTCAGGCG	
rasR-F	5′-ATGAAAAATTGGCAAGAAGATCTGCTGGAT	Complementary *rasR*
rasR-R	5′-TGTCTCCCGATCGCCAAAAAGCACCCTC	
pBBR-mcherry-F	5′-ATCCAGCAGATCTTCTTGCCAATTTTTCATCTGCACCCTCCTCCTCGCTG	Construction of P*rasI-mCherry*
pBBR-mcherry-R	5′-GAGGGTGCTTTTTGGCGATCGGGAGACAAGGAGGGTGCAGATGGTGAGCA	
RS rasR-F	5′-CCCTTGCTCACCATCTGCACCCTCCTTGTCTCCCGATCGCCAAAAAGCAC	Construction of *rasR*-P*rasI-mCherry*
RS rasR-R	5′-GCAGCGAGGAGGAGGGTGCAGATGAAAAATTGGCAAGAAGATCTGCTGGA	
rasR check F	5′-CTCCCACTTGAAGCCCTCGG	
rasR check R	5′-CGTCTGGTCCGACCGGTTGT	
pBBR-solR mcherry F	5′-GTGATACGCGTCCTGGAAGCCTGGTCCCATCTGCACCCTCCTCCTCGCTG	Construction of P*soll-mCherry*
pBBR-solR mcherry R	5′-ATGCAGACATTCATTCATGGCGGCGGGAGGAGGGTGCAGATGGTGAGCA	
soll promoter F	5′-CTCGCCCTTGCTCACCATCTGCACCCTCCTCCCGCCGCCATGAATGAAT	
soll promoter R	5′-GTCAAGGCGATCGCCATCGGACTGATCTAGCGCATGCCACTGTGAACAGC	
solR mCherry F	5′-GCACGGGCTGTTCACAGTGGCATGCGCTAGATCAGTCCGATGGCGATCGC	
solR mCherry R	5′-AATCATCTGCAGCGAGGAGGAGGGTGCAGATGGGACCAGGCTTCCAGGAC	
solR Check F	5′-GCTCACGGTCACAAGAAGA	

(Continued on next page)

TABLE 2 (Continued)

Strains/plasmids/primers	Characteristics	Source or usage
solR Check R	5′-GGCTTTGACTACTGCTGCTAC	
recA-F	5′-CACCGAAGCGTAGAACTTGA	qRT-PCR
recA-R	5′-CCAACTGCCTGGTGATCTT	qRT-PCR
AC251_22465-F	5′-CAATCTTGGTCGCTATCG	qRT-PCR
AC251_22465-R	5′-ATCAAATGCTTCGTGTCG	qRT-PCR
AC251_19280-F	5′-GCAGGACTTCACCAACTG	qRT-PCR
AC251_19280-R	5′-CATCGGCATTGTTCTTCAC	qRT-PCR
AC251_00725-F	5′-ATCAAGATCCAGGTGTCG	qRT-PCR
AC251_00725-R	5′-GTCGTTGTAGTCGTTGTC	qRT-PCR
AC251_00730-F	5′-TTGACTACTGCTGCTACG	qRT-PCR
AC251_00730-R	5′-CTCATCACGGATGGACAC	qRT-PCR
AC251_23955-F	5′-GGCTTCCTTGATGTCCTG	qRT-PCR
AC251_23955-R	5′-CGAGTTCTCCAACCAGAC	qRT-PCR
AC251_19340-F	5′-CGATTCCGTCATCCATATC	qRT-PCR
AC251_19340-R	5′-GATCAGCCGTTCATTGAG	qRT-PCR
AC251_17135-F	5′-CAAGCATTCGACCAAGTT	qRT-PCR
AC251_17135-R	5′-GAGTACCAAGCACAATCAG	qRT-PCR
AC251_23985-F	5′-GATTTCAGTGCCCAGAGT	qRT-PCR
AC251_23985-R	5′-ACGCCATTTCAGTTCCTT	qRT-PCR
AC251_22035-F	5′-CGAGTGCTGACAGATTCA	qRT-PCR
AC251_22035-R	5′-GGATTGACCGTGATGAGAT	qRT-PCR
AC251_25945-F	5′-GCATTACCAACACGGAAG	qRT-PCR
AC251_25945-R	5′-CGATAAAGCGATCTGGAAA	qRT-PCR

mL gentamicin. AHL derivatives were used as necessary at a final concentration of 100 nM, unless otherwise indicated.

Mutant and plasmid construction. Mutants with deletion of *rasI*, *rasR*, *soll*, *solR*, *phcB*, and *phcA* were derived from *R. solanacearum* EP1 by a homologous recombination-based two-step allelic exchange approach (54). Briefly, DNA fragments of about 500 to 800 bp flanking the gene of interest were PCR amplified and cloned into the pK18mobsacB vector by standard restriction enzyme-based techniques. The resultant constructs were transformed into *E. coli* DH5α, and the transformants were selected on LB agar containing gentamicin. The primers for PCR amplifications are listed in Table 2. The knockout plasmids were confirmed by DNA sequencing and introduced into *R. solanacearum* through triparental mating with the helper strain *E. coli* HB101(pRK2013). Merodiploids were selected by plating on CTG plates containing gentamicin, and deletion mutants were then selected on CTG agar containing 10 to 15% sucrose. The complemented Δ*rasI*(*rasI*) and Δ*rasR*(*rasR*) strains were derived by in *trans* expression of corresponding WT genes in the Δ*rasI* and Δ*rasR* deletion mutants, respectively. The coding sequences of *rasI* and *rasR* were amplified by PCR using specific primer pairs (Table 2) that were cloned into the pBBR1-MCS-2/5 vector by standard techniques. The resultant constructs were transformed into *E. coli* DH5α, purified, and electroporated into the *R. solanacearum* Δ*rasI* and Δ*rasR* deletion mutants. All deletion mutations and complemented mutants were confirmed by PCR and DNA sequencing.

Construction of the RasR-P*rasI*-mCherry reporter plasmid (pYJL01) was done by *E. coli* DH5α-mediated assembly (55). Briefly, the DNA fragments containing the predicted RasI promoter and the RasR ORF were amplified by corresponding primers listed in Table 2 using strain EP1 genomic DNA as the template. The linearized pBBR-mCherry fragment was generated by PCR amplification using the plasmid pLL1 as the template (56). Two DNA fragments contain at least 25 bp of homologous overlap, which is required for *E. coli* DH5α-mediated assembly. Transformants were selected on LB plates containing 10 μg/mL gentamicin and confirmed by DNA sequencing with the RasR-Check-F and RasR-Check-R primers (Table 2). The confirmed construct was electroporated into *P. putida* F1 to generate the reporter strain YJL01. To detect the signal produced by Soll, we decided to construct a *soll* signal-specific reporter using the same method, and a *solR*-P*soll*-mCherry reporter construct (pYJL02) by fusing the *soll* promoter with the ORF of the mCherry gene, which together with the *solR* coding sequence were cloned in the expression vector pBBPgdh and introduced in the non-QS heterologous host *Pseudomonas putida* F1 to produce the reporter strain YJL02 (Fig. S1). The primers used for construction of the reporter strains are listed in Table 2.

Bioassay of AHL signals. The AHL bioassay was performed with the reporter strain YJL01 or YJL02 using the following protocol. The bacterial cell-free culture supernatants were prepared by centrifugation (20,000 $\times$ *g*, 30 min, 4°C) to remove cells, which were then extracted twice with an equal volume of acidified ethyl acetate (0.1 mL of glacial acetic acid/L). Ethyl acetate extracts were added to 16-mL glass tubes, and ethyl acetate was removed by evaporation under a gentle stream of N_2 gas. Overnight culture of the reporter strain YJL01 or YJL02 was diluted to an OD_{600} of 0.05 and was added to the tubes containing the signal solution in a final volume of 1.0 mL. The tubes were then incubated for 16 h at 30°C

with shaking, and then fluorescence was measured as described previously (56). Corresponding synthetic AHLs were used to prepare standard curves.

Purification of AHLs from *R. solanacearum* EP1. To purify the AHL signals synthesized by RasI, *R. solanacearum* EP1 was inoculated in 1 L of CTG liquid medium and cultured until it reached an OD_{600} of about 2.0. The bacterial cells were removed by centrifugation, and supernatants were extracted with two equal volumes of 0.1% acidified ethyl acetate. The concentrated extracts were fractionated by the C_{18} reverse-phase (RP) HPLC column, as described previously (56). Each 1-mL fraction was collected and assayed by using the reporter strain YJL01, as described in the previous section. The bulk of the active fractions were collected, dried, and separated by isocratic HPLC with 80% methanol. Fractions were collected, dried, and tested as described in the text. Two purified active fractions and synthetic *N*-(3-hydroxydodecanoyl)-HSL and *N*-(3-hydroxytetradecanoyl)-HSL were analyzed by LC-MS/MS in a Waters Acquity ultraperformance liquid chromatography (UPLC) C_{18} RP column (1.7 μm, 2.1 mm by 30 mm) with a Thermo Linear Trap Quadrupole Orbitrap MS System (collision energy = 40 eV, cone = 35 V). Using the same approach, we also purified the AHL signals from the *solI* mutant of *R. solanacearum* EP1 and found the same active fractions as those from WT EP1.

RNA preparation, RNA-seq, data analysis, and qRT-PCR. Total RNA was extracted with Eastep Super Total RNA extraction kit (Promega, Madison, WI, USA) from 1-mL cultures of *R. solanacearum* strains when the OD_{600} reached at about 1.0. Ribosomal RNAs were removed from the prepared total RNA samples with the RiboZero rRNA removal kit (for Gram-negative bacteria) (Illumina, Madison, WI, USA). cDNA library preparation and RNA sequencing were performed by Novogene (Beijing, China) using Illumina HiSeq 2500 single-end reads. Clean reads were obtained by removing adaptors, unknown nucleotides, and low-quality reads. In addition, clean reads were aligned to the *R. solanacearum* EP1 genome (GenBank accession no. CP015115.1 and CP015116.1), using Bowtie2 v.2.2.3 (57). For expression quantification, the number of read pairs aligned to each gene was counted using the featureCounts tool from the subread package v.0.30 (27). Additionally, the FPKM (fragments per kilobase of transcript per million mapped reads) method was used to normalize the level of gene expression (58), Moreover, DESeq2 was used for differential expression analysis (59), using the Benjamini-Hochberg adjustment for multiple comparisons and a false-discovery rate of <0.05. The differentially expressed genes (DEGs) were then subjected to enrichment analysis through Gene Ontology (GO) and Kyoto Encyclopedia of Genes and Genomes (KEGG) pathway analyses.

RNA samples were reverse transcribed into cDNA using HiScript III RT SuperMix for quantitative PCR (qPCR) (Vazyme). qRT-PCR analyses were performed with ChamQ Universal SYBR qPCR master mix (Vazyme). The gene expression level of *recA* was used as a control for qRT-PCR analysis. The primers used in qRT-PCR analysis are listed in Table 2. The absolute values of relative expression of target genes were calculated using the threshold cycle ($2^{-\Delta\Delta CT}$) method, as described previously (60). The RNA samples were extracted twice, and each time, qRT-PCR was performed in triplicate.

Twitching and swimming assay. CTG plates with 1.6% Difco agar were used for analysis of twitching motilities (6), and swimming motility soft agar (61) was used for analysis of swimming motilities. Both motility tests were carried out by inoculation of a 1-μL bacterial suspension (OD_{600} = 0.1) at the plate center. After inoculation, plates were incubated at 30°C for 24 h for the twitching assay and 48 h for the swimming assay. When the layered edges with multiple irregular projections appeared in the WT strain, twitching motility was observed, and images were taken using a Leica microsystem (Leica Microscopy, Wetzlar, Germany). Swimming motility were measured, and images were obtained by using a ChemiDoc XRS system (Bio-Rad, Hercules, CA). The experiments were repeated at least twice in triplicate.

Cellulase activity and biofilm assay. Bacterial suspensions were prepared from overnight cultures in CTG rich broth and adjusted to an OD_{600} of 1.5. In addition, 20 μL of adjusted bacterial suspensions was placed into the middle hole of previously prepared carboxymethyl cellulose (0.2%) plates (62). Spotted plates were incubated at 28°C overnight for 24 h. Plates were stained for 15 min with 20 mL of 0.1% (wt/vol) Congo red, and then plates were soaked with 1 M NaCl for 10 min. After clear zones appeared in the solution, the diameters of the transparent circles were observed and measured. The experiments were repeated at least twice in triplicate.

The biofilm assay was performed according to the method described previously, with slight modification (62, 63). In brief, 1 μL of bacterial overnight culture was added to 16-mL glass tubes containing 1 mL CTG liquid medium and statically cultured in a constant-temperature incubator at 28°C for 48 h. After staining with 0.1% crystal violet for 10 min at room temperature, the stained biofilm samples were rinsed several times with water and dissolved in ethanol. Biofilm quantification was performed by measuring the absorbance at 570 nm. The experiment was repeated at least three times, each time with three replicates.

Bacterial pathogenicity assay. For the virulence assay, 1-month-old root tip-cutting eggplant seedlings were inoculated by soil soaking with 40-mL bacterial suspensions in Milli-Q water ($\sim 10^8$ CFU/mL), and the same volume of Milli-Q water was used as the negative control. The inoculated plants were then maintained in the greenhouse (30 $\pm$ 2°C, 90% $\pm$ 5% relative humidity). Each treatment contained 10 plants, and the experiment was repeated three times. Wilting symptoms were recorded daily based on the following disease index scale: 0, no wilt;, 1, 1 to 25% of leaves wilted; 2, 26 to $\sim$50% of leaves wilted; 3, 51 to $\sim$75% of leaves wilted; 4, $>$75% of leaves wilted; 5, plant died (64).

To determine bacterial systemic infection ability and survival around the inoculation point, the method described by Shen et al. (62) was followed, with slight modification. In brief, about 0.1 g of eggplant roots or stems 3 cm from the root (1 g) were collected at 3, 5, 7, and 10 days postinoculation (dpi), which were cut in small pieces and placed in tubes containing 1 mL of Milli-Q water with shaking. After 1 h of incubation at room temperature, serial dilutions were prepared, and the corresponding CTG

medium was coated with them to measure viable bacterial cells (CFU) (62). Each treatment contained 10 plants, and the experiment was repeated three times.

Bacterial sensitivity assay on hydrogen peroxide. To test bacterial resistance to hydrogen peroxide, the method described previously was used with minor modifications (65). *R. solanacearum* cells in CTG liquid medium were cultured for 24 h, and 100 μL was taken and inoculated into 1 mL fresh CTG medium containing different concentrations of hydrogen peroxide as indicated. At 24 h postinoculation, aliquots of the cultures were taken, diluted, and plated on CTG agar plates. The plates were incubated at 28°C for 24 h prior to counting bacterial colony numbers. The experiment was repeated twice in triplicate.

Statistical analysis. All of the experiments were repeated at least twice in triplicate or as otherwise indicated. Statistical significance was determined with a two-tailed *t* test for comparison between two treatments and one-way analysis of variance (ANOVA) for comparison between multiple treatments, where a *P* value of <0.05 was considered statistically significant. *P* values for all respective analyses are indicated in the figure legends.

Data availability. The raw data from transcriptome analyses were deposited in the NCBI Sequence Read Archive (SRA) under accession no. PRJNA833281.

SUPPLEMENTAL MATERIAL

Supplemental material is available online only.

SUPPLEMENTAL FILE 1, PDF file, 1 MB.

SUPPLEMENTAL FILE 2, XLSX file, 0.1 MB.

SUPPLEMENTAL FILE 3, XLSX file, 0.1 MB.

ACKNOWLEDGMENTS

This work was supported by the grants from Guangdong Forestry Science and Technology Innovation Project (2018KJCX009 and 2020KJCX009), the Key Realm R&D Program of Guangdong Province (2020B0202090001 and 2018B020205003), and the Basic Research and Applied Basic Research Program of Guangdong Province (2020A1515110111), National Natural Science Foundation of China (31900076), and Guangzhou Basic Research Program (202102020853).

J.Y., L.L., and L.Z. conceived the study. J.Y. and P.L. did most of the experiments. X.W., M.Z., H.S., G.Y., X.C., H.W., and X.Z. provided technical assistance. J.Y., L.L., P.L., and L.Z. analyzed the data. L.L. and L.Z. supervised the study and wrote the manuscript, with input from J.Y. and P.L. All authors discussed the results and commented on the manuscript.

We declare no conflict of interest.

REFERENCES

1. Genin S, Denny TP. 2012. Pathogenomics of the *Ralstonia solanacearum* species complex. Annu Rev Phytopathol 50:67–89. https://doi.org/10.1146/annurev-phyto-081211-173000.
2. Hayward AC. 1991. Biology and epidemiology of bacterial wilt caused by *Pseudomonas solanacearum*. Annu Rev Phytopathol 29:65–87. https://doi.org/10.1146/annurev.py.29.090191.000433.
3. Mansfield J, Genin S, Magori S, Citovsky V, Sriariyanum M, Ronald P, Dow M, Verdier V, Beer SV, Machado MA, Toth I, Salmond G, Foster GD. 2012. Top 10 plant pathogenic bacteria in molecular plant pathology. Mol Plant Pathol 13:614–629. https://doi.org/10.1111/j.1364-3703.2012.00804.x.
4. Genin S. 2010. Molecular traits controlling host range and adaptation to plants in *Ralstonia solanacearum*. New Phytol 187:920–928. https://doi.org/10.1111/j.1469-8137.2010.03397.x.
5. Lowe-Power TM, Khokhani D, Allen C. 2018. How *Ralstonia solanacearum* exploits and thrives in the flowing plant xylem environment. Trends Microbiol 26:929–942. https://doi.org/10.1016/j.tim.2018.06.002.
6. Corral J, Sebastia P, Coll NS, Barbe J, Aranda J, Valls M. 2020. Twitching and swimming motility play a role in *Ralstonia solanacearum* pathogenicity. mSphere 5:e00740-19. https://doi.org/10.1128/mSphere.00740-19.
7. Deslandes L, Genin S. 2014. Opening the *Ralstonia solanacearum* type III effector tool box: insights into host cell subversion mechanisms. Curr Opin Plant Biol 20:110–117. https://doi.org/10.1016/j.pbi.2014.05.002.
8. Moleleki LN, Pretorius RG, Tanui CK, Mosina G, Theron J. 2017. A quorum sensing-defective mutant of *Pectobacterium carotovorum ssp. brasiliense* 1692 is attenuated in virulence and unable to occlude xylem tissue of susceptible potato plant stems. Mol Plant Pathol 18:32–44. https://doi.org/10.1111/mpp.12372.
9. Mori Y, Hosoi Y, Ishikawa S, Hayashi K, Asai Y, Ohnishi H, Shimatani M, Inoue K, Ikeda K, Nakayashiki H, Nishimura Y, Ohnishi K, Kiba A, Kai K, Hikichi Y. 2018. Ralfuranones contribute to mushroom-type biofilm formation by *Ralstonia solanacearum* strain OE1-1. Mol Plant Pathol 19:975–985. https://doi.org/10.1111/mpp.12583.
10. Papenfort K, Bassler BL. 2016. Quorum sensing signal-response systems in Gram-negative bacteria. Nat Rev Microbiol 14:576–588. https://doi.org/10.1038/nrmicro.2016.89.
11. Whiteley M, Diggle SP, Greenberg EP. 2017. Progress in and promise of bacterial quorum sensing research. Nature 551:313–320. https://doi.org/10.1038/nature24624.
12. Dang HT, Komatsu S, Masuda H, Enomoto K. 2017. Characterization of luxI and luxR protein homologs of N-acyl homoserine lactone-dependent quorum sensing system in *Pseudoalteromonas* sp. 520P1. Mar Biotechnol (NY) 19:1–10. https://doi.org/10.1007/s10126-016-9726-4.
13. Schaefer AL, Greenberg EP, Oliver CM, Oda Y, Huang JJ, Bittan-Banin G, Peres CM, Schmidt S, Juhaszova K, Sufrin JR, Harwood CS. 2008. A new class of homoserine lactone quorum-sensing signals. Nature 454:595–599. https://doi.org/10.1038/nature07088.
14. Abisado RG, Benomar S, Klaus JR, Dandekar AA, Chandler JR. 2018. Bacterial quorum sensing and microbial community interactions. mBio 9:e01749-18. https://doi.org/10.1128/mBio.01749-18.
15. Kostylev M, Kim DY, Smalley NE, Salukhe I, Greenberg EP, Dandekar AA. 2019. Evolution of the *Pseudomonas aeruginosa* quorum-sensing hierarchy. Proc Natl Acad Sci U S A 116:7027–7032. https://doi.org/10.1073/pnas.1819796116.

16. Lee J, Zhang L. 2015. The hierarchy quorum sensing network in *Pseudomonas aeruginosa*. Protein Cell 6:26–41. https://doi.org/10.1007/s13238-014-0100-x.
17. Chandler JR, Duerkop BA, Hinz A, West TE, Herman JP, Churchill ME, Skerrett SJ, Greenberg EP. 2009. Mutational analysis of *Burkholderia thailandensis* quorum sensing and self-aggregation. J Bacteriol 191:5901–5909. https://doi.org/10.1128/JB.00591-09.
18. Cornforth DM, Popat R, McNally L, Gurney J, Scott-Phillips TC, Ivens A, Diggle SP, Brown SP. 2014. Combinatorial quorum sensing allows bacteria to resolve their social and physical environment. Proc Natl Acad Sci U S A 111:4280–4284. https://doi.org/10.1073/pnas.1319175111.
19. Flavier AB, Ganova-Raeva LM, Schell MA, Denny TP. 1997. Hierarchical autoinduction in *Ralstonia solanacearum*: control of acyl-homoserine lactone production by a novel autoregulatory system responsive to 3-hydroxypalmitic acid methyl ester. J Bacteriol 179:7089–7097. https://doi.org/10.1128/jb.179.22.7089-7097.1997.
20. Flavier AB, Clough SJ, Schell MA, Denny TP. 1997. Identification of 3-hydroxypalmitic acid methyl ester as a novel autoregulator controlling virulence in *Ralstonia solanacearum*. Mol Microbiol 26:251–259. https://doi.org/10.1046/j.1365-2958.1997.5661945.x.
21. Kai K, Ohnishi H, Shimatani M, Ishikawa S, Mori Y, Kiba A, Ohnishi K, Tabuchi M, Hikichi Y. 2015. Methyl 3-hydroxymyristate, a diffusible signal mediating phc quorum sensing in *Ralstonia solanacearum*. Chembiochem 16:2309–2318. https://doi.org/10.1002/cbic.201500456.
22. Ujita Y, Sakata M, Yoshihara A, Hikichi Y, Kai K. 2019. Signal production and response specificity in the phc quorum sensing systems of *Ralstonia solanacearum* species complex. ACS Chem Biol 14:2243–2251.
23. Brumbley SM, Carney BF, Denny TP. 1993. Phenotype conversion in *Pseudomonas solanacearum* due to spontaneous inactivation of PhcA, a putative LysR transcriptional regulator. J Bacteriol 175:5477–5487. https://doi.org/10.1128/jb.175.17.5477-5487.1993.
24. Bhatt G, Denny TP. 2004. *Ralstonia solanacearum* iron scavenging by the siderophore staphyloferrin B is controlled by PhcA, the global virulence regulator. J Bacteriol 186:7896–7904. https://doi.org/10.1128/JB.186.23.7896-7904.2004.
25. Genin S, Brito B, Denny TP, Boucher C. 2005. Control of the *Ralstonia solanacearum* type III secretion system (Hrp) genes by the global virulence regulator PhcA. FEBS Lett 579:2077–2081. https://doi.org/10.1016/j.febslet.2005.02.058.
26. Huang J, Carney BF, Denny TP, Weissinger AK, Schell MA. 1995. A complex network regulates expression of eps and other virulence genes of *Pseudomonas solanacearum*. J Bacteriol 177:1259–1267. https://doi.org/10.1128/jb.177.5.1259-1267.1995.
27. Liao Y, Smyth GK, Shi W. 2014. featureCounts: an efficient general purpose program for assigning sequence reads to genomic features. Bioinformatics 30:923–930. https://doi.org/10.1093/bioinformatics/btt656.
28. Puri AW, Schaefer AL, Fu Y, Beck D, Greenberg EP, Lidstrom ME. 2017. Quorum sensing in a methane-oxidizing bacterium. J Bacteriol 199:e00773-16. https://doi.org/10.1128/JB.00773-16.
29. Puri AW, Mevers E, Ramadhar TR, Petras D, Liu D, Piel J, Dorrestein PC, Greenberg EP, Lidstrom ME, Clardy J. 2018. Tundrenone: an atypical secondary metabolite from bacteria with highly restricted primary metabolism. J Am Chem Soc 140:2002–2006. https://doi.org/10.1021/jacs.7b12240.
30. Dong YH, Wang LH, Xu JL, Zhang HB, Zhang XF, Zhang LH. 2001. Quenching quorum-sensing-dependent bacterial infection by an N-acyl homoserine lactonase. Nature 411:813–817. https://doi.org/10.1038/35081101.
31. Wang LH, Weng LX, Dong YH, Zhang LH. 2004. Specificity and enzyme kinetics of the quorum-quenching N-acyl homoserine lactone lactonase (AHL-lactonase). J Biol Chem 279:13645–13651. https://doi.org/10.1074/jbc.M311194200.
32. Mellbye BL, Spieck E, Bottomley PJ, Sayavedra-Soto LA. 2017. Acyl-homoserine lactone production in Nitrifying bacteria of the genera *Nitrosospira*, *Nitrobacter*, and *Nitrospira* identified via a survey of putative quorum-sensing genes. Appl Environ Microbiol 83:e01540-17. https://doi.org/10.1128/AEM.01540-17.
33. Liu H, Kang Y, Genin S, Schell MA, Denny TP. 2001. Twitching motility of *Ralstonia solanacearum* requires a type IV pilus system. Microbiology (Reading) 147:3215–3229. https://doi.org/10.1099/00221287-147-12-3215.
34. Aoun N, Tauleigne L, Lonjon F, Deslandes L, Vailleau F, Roux F, Berthome R. 2017. Quantitative disease resistance under elevated temperature: genetic basis of new resistance mechanisms to *Ralstonia solanacearum*. Front Plant Sci 8:1387. https://doi.org/10.3389/fpls.2017.01387.
35. Lohou D, Turner M, Lonjon F, Cazale AC, Peeters N, Genin S, Vailleau F. 2014. HpaP modulates type III effector secretion in *Ralstonia solanacearum* and harbours a substrate specificity switch domain essential for virulence. Mol Plant Pathol 15:601–614. https://doi.org/10.1111/mpp.12119.
36. Chugani S, Greenberg EP. 2010. LuxR homolog-independent gene regulation by acyl-homoserine lactones in *Pseudomonas aeruginosa*. Proc Natl Acad Sci U S A 107:10673–10678. https://doi.org/10.1073/pnas.1005909107.
37. Mukherjee S, Moustafa D, Smith CD, Goldberg JB, Bassler BL. 2017. The RhlR quorum-sensing receptor controls *Pseudomonas aeruginosa* pathogenesis and biofilm development independently of its canonical homoserine lactone autoinducer. PLoS Pathog 13:e1006504. https://doi.org/10.1371/journal.ppat.1006504.
38. Li P, Wang D, Yan J, Zhou J, Deng Y, Jiang Z, Cao B, He Z, Zhang L. 2016. Genomic analysis of phylotype I strain EP1 reveals substantial divergence from other strains in the *Ralstonia solanacearum* species complex. Front Microbiol 7:1719.
39. Liu H, Zhang S, Schell MA, Denny TP. 2005. Pyramiding unmarked deletions in *Ralstonia solanacearum* shows that secreted proteins in addition to plant cell-wall-degrading enzymes contribute to virulence. Mol Plant Microbe Interact 18:1296–1305. https://doi.org/10.1094/MPMI-18-1296.
40. Weller-Stuart T, Toth I, Maayer PD, Coutinho T. 2017. Swimming and twitching motility are essential for attachment and virulence of Pantoea ananatis in onion seedlings. Mol Plant Pathol 18:734–745. https://doi.org/10.1111/mpp.12432.
41. Ferreira RM, Moreira LM, Ferro JA, Soares M, Laia ML, Varani AM, de Oliveira J, Ferro M. 2016. Unravelling potential virulence factor candidates in *Xanthomonas citri*. subsp. *citri* by secretome analysis. PeerJ 4:e1734. https://doi.org/10.7717/peerj.1734.
42. Otten C, Buttner D. 2021. HrpB4 from *Xanthomonas campestris* pv. vesicatoria acts similarly to SctK proteins and promotes the docking of the predicted sorting platform to the type III secretion system. Cell Microbiol 23:e13327. https://doi.org/10.1111/cmi.13327.
43. Tans-Kersten J, Huang H, Allen C. 2001. *Ralstonia solanacearum* needs motility for invasive virulence on tomato. J Bacteriol 183:3597–3605. https://doi.org/10.1128/JB.183.12.3597-3605.2001.
44. Buddenhagen DA, Haeff AV, Smith GF, Oster G, Oster GK. 1962. Observations of ruby-laser beam-intensity patterns with dye-sensitized photopolymers. Proc Natl Acad Sci U S A 48:303–305. https://doi.org/10.1073/pnas.48.2.303.
45. Palleroni NJ, Doudoroff M. 1971. Phenotypic characterization and deoxyribonucleic acid homologies of *Pseudomonas solanacearum*. J Bacteriol 107:690–696. https://doi.org/10.1128/jb.107.3.690-696.1971.
46. Salanoubat M, Genin S, Artiguenave F, Gouzy J, Mangenot S, Arlat M, Billault A, Brottier P, Camus JC, Cattolico L, Chandler M, Choisne N, Claudel-Renard C, Cunnac S, Demange N, Gaspin C, Lavie M, Moisan A, Robert C, Saurin W, Schiex T, Siguier P, Thebault P, Whalen M, Wincker P, Levy M, Weissenbach J, Boucher CA. 2002. Genome sequence of the plant pathogen *Ralstonia solanacearum*. Nature 415:497–502. https://doi.org/10.1038/415497a.
47. Clough SJ, Lee KE, Schell MA, Denny TP. 1997. A two-component system in *Ralstonia* (*Pseudomonas*) *solanacearum* modulates production of PhcA-regulated virulence factors in response to 3-hydroxypalmitic acid methyl ester. J Bacteriol 179:3639–3648. https://doi.org/10.1128/jb.179.11.3639-3648.1997.
48. Ahator SD, Zhang L. 2019. Small is mighty—chemical communication systems in *Pseudomonas aeruginosa*. Annu Rev Microbiol 73:559–578. https://doi.org/10.1146/annurev-micro-020518-120044.
49. Dou Y, Song F, Guo F, Zhou Z, Zhu C, Xiang J, Huan J. 2017. *Acinetobacter baumannii* quorum-sensing signalling molecule induces the expression of drug-resistance genes. Mol Med Rep 15:4061–4068. https://doi.org/10.3892/mmr.2017.6528.
50. Oh MH, Choi CH. 2015. Role of luxIR homologue anoIR in *Acinetobacter nosocomialis* and the effect of virstatin on the expression of anoR gene. J Microbiol Biotechnol 25:1390–1400. https://doi.org/10.4014/jmb.1504.04069.
51. Ghani MI, Ali A, Atif MJ, Ali M, Amin B, Anees M, Khurshid H, Cheng Z. 2019. Changes in the soil microbiome in eggplant monoculture revealed by high-throughput Illumina miSeq sequencing as influenced by raw garlic stalk amendment. Int J Mol Sci 20:2125. https://doi.org/10.3390/ijms20092125.
52. Li H, Ding X, Chen C, Zheng X, Han H, Li C, Gong J, Xu T, Li QX, Ding GC, Li J. 2019. Enrichment of phosphate solubilizing bacteria during late developmental stages of eggplant (Solanum melongena L.). FEMS Microbiol Ecol 95:fiz023. https://doi.org/10.1093/femsec/fiz023.
53. Hendrick CA, Sequeira L. 1984. Lipopolysaccharide-defective mutants of the wilt pathogen *Pseudomonas solanacearum*. Appl Environ Microbiol 48:94–101. https://doi.org/10.1128/aem.48.1.94-101.1984.
54. Li P, Yin W, Yan J, Chen Y, Fu S, Song S, Zhou J, Lyu M, Deng Y, Zhang LH. 2017. Modulation of inter-kingdom communication by phcBSR quorum sensing system in *Ralstonia solanacearum* phylotype I strain GMI1000. Front Microbiol 8:1172. https://doi.org/10.3389/fmicb.2017.01172.

55. Kostylev M, Otwell AE, Richardson RE, Suzuki Y. 2015. Cloning should be simple: *Escherichia coli* DH5alpha-mediated assembly of multiple DNA fragments with short end homologies. PLoS One 10:e0137466. https://doi.org/10.1371/journal.pone.0137466.
56. Liao L, Schaefer AL, Coutinho BG, Brown P, Greenberg EP. 2018. An aryl-homoserine lactone quorum-sensing signal produced by a dimorphic prosthecate bacterium. Proc Natl Acad Sci U S A 115:7587–7592. https://doi.org/10.1073/pnas.1808351115.
57. Langmead B, Salzberg SL. 2012. Fast gapped-read alignment with Bowtie 2. Nat Methods 9:357–359. https://doi.org/10.1038/nmeth.1923.
58. Trapnell C, Roberts A, Goff L, Pertea G, Kim D, Kelley DR, Pimentel H, Salzberg SL, Rinn JL, Pachter L. 2012. Differential gene and transcript expression analysis of RNA-seq experiments with TopHat and Cufflinks. Nat Protoc 7:562–578. https://doi.org/10.1038/nprot.2012.016.
59. Love MI, Huber W, Anders S. 2014. Moderated estimation of fold change and dispersion for RNA-seq data with DESeq2. Genome Biol 15:550. https://doi.org/10.1186/s13059-014-0550-8.
60. Livak KJ, Schmittgen TD. 2001. Analysis of relative gene expression data using real-time quantitative PCR and the 2(−Delta Delta C(T)) method. Methods 25:402–408. https://doi.org/10.1006/meth.2001.1262.
61. Shi Z, Wang Q, Li Y, Liang Z, Xu L, Zhou J, Cui Z, Zhang LH. 2019. Putrescine is an intraspecies and interkingdom cell-cell communication signal modulating the virulence of *Dickeya* zeae. Front Microbiol 10:1950. https://doi.org/10.3389/fmicb.2019.01950.
62. Shen F, Yin W, Song S, Zhang Z, Ye P, Zhang Y, Zhou J, He F, Li P, Deng Y. 2020. *Ralstonia solanacearum* promotes pathogenicity by utilizing l-glutamic acid from host plants. Mol Plant Pathol 21:1099–1110. https://doi.org/10.1111/mpp.12963.
63. Dong YH, Zhang XF, An SW, Xu JL, Zhang LH. 2008. A novel two-component system BqsS-BqsR modulates quorum sensing-dependent biofilm decay in *Pseudomonas aeruginosa*. Commun Integr Biol 1:88–96. https://doi.org/10.4161/cib.1.1.6717.
64. Yang L, Li S, Qin X, Jiang G, Chen J, Li B, Yao X, Liang P, Zhang Y, Ding W. 2017. Exposure to umbelliferone reduces *Ralstonia solanacearum* biofilm formation, transcription of type III secretion system regulators and effectors and virulence on tobacco. Front Microbiol 8:1234. https://doi.org/10.3389/fmicb.2017.01234.
65. Flores-Cruz Z, Allen C. 2011. Necessity of OxyR for the hydrogen peroxide stress response and full virulence in *Ralstonia solanacearum*. Appl Environ Microbiol 77:6426–6432. https://doi.org/10.1128/AEM.05813-11.